JACS
JOURNAL OF THE AMERICAN CHEMICAL SOCIETY
Communication
pubs.acs.org/JACS

Cation-Dependent Magnetic Ordering and Room-Temperature Bistability in Azido-Bridged Perovskite-Type Compounds

Xin-Hua Zhao,[†,§] Xing-Cai Huang,[†,§] Shao-Liang Zhang,[†] Dong Shao,[†] Hai-Yan Wei,*[,‡] and Xin-Yi Wang*[,†]

[†]State Key Laboratory of Coordination Chemistry, School of Chemistry and Chemical Engineering, Nanjing University, Nanjing, 210093, China

[‡]Jiangsu Key Laboratory of Biofunctional Materials, School of Chemistry and Materials Science, Nanjing Normal University, Nanjing, 210097, China

Supporting Information

ABSTRACT: A series of end-to-end azido-bridged perovskite-type compounds $[(CH_3)_nNH_{4-n}][Mn(N_3)_3]$ (n = 1−4) were synthesized and characterized. Structural phase transitions indicating the general lattice flexibility were observed and confirmed by the crystal structures of different phases. These materials show cation-dependent magnetic ordering at up to 92 K and magnetic bistability near room temperature.

Molecular bistability has invoked intense interest in the molecular materials community because of its great potential for application in sensors, displays, and switching devices.[1,2] Outstanding examples of this behavior are found in spin crossover materials,[3] charge-transfer complexes,[4] organic radicals with monomer−dimer transition,[5−7] compounds with spin-Peierls-type transition,[8] and complexes with dynamic coordination environments.[9] In the case of bulk materials, the bistability is often accompanied with a structural phase transtion. In this regard, the inorganic perovskite ABX_3-type compounds are remarkable as they are well-known to be susceptible to sequential structural phase transitions accompanied by intriguing properties such as ferroelectricity as found in $BaTiO_3$, multiferroics exhibited by $BiFeO_3$, and giant magnetoresistance effects in $La_{1-x}Ca_xMnO_3$.[10−12]

Recently, metal−organic frameworks (MOFs) of perovskite-type structures have come into the forefront of the aforementioned areas with representatives being the multiferroic formato-bridged MOFs $[(CH_3)_2NH_2][M(HCOO)_3]$ ($M = Mn^{2+}$, Co^{2+}, Ni^{2+}, Zn^{2+}).[13−15] Magnetic coupling through formate and order−disorder hydrogen-bonding transitions of the $(CH_3)_2NH_2^+$ cation lead to magnetic ordering below 8.5−35.6 K and electric ordering below 150−185 K.[14,15] Specific cations such as free radicals and those with O−H groups have been proposed to increase the magnetic communication and the hydrogen-bond enengy, and thus the magnetic and electric critical temperatures,[15f] but it is difficult for these cations, especially the radicals, to fit into the small cavity of the framework. It is worth noting that different alkylammonium cations were found to have little influence on the physical properties of the resulting complexes with similar structures.[14b]

In terms of the desired characteristics, the azide ligand presents several advantages: (1) The azide and formate ions are comparable for obtaining magnetic MOFs with similar structures.[14c] For example, the $[(CH_3)_2NH_2][M(HCOO)_3]$ compounds and the azide analog $[(CH_3)_4N][Mn(N_3)_3]$ reported by Mautner and Rojo have very similar distorted perovskite architectures.[16] (2) In terms of properties, the stronger magnetic coupling transmitted by azide can lead to materials with much higher T_c values.[14c] (3) Due to the cylindrical distribution of the negative charges and high electron density on both the terminal N atoms, azide can be used as effective building blocks to form hydrogen-bonding interactions, which might be used to tune the critical temperature of the structural phase transition.[17]

Herein, we demonstrate the generality and flexibility of the perovskite architecture for the azido-bridged MOFs by the series of compounds $[(CH_3)_nNH_{4-n}][Mn(N_3)_3]$ (n = 1 (**1**), 2 (**2**), 3 (**3**), and 4 (**4**)). Single crystal X-ray analysis at numerous temperatures, thermal analyses, and magnetic measurements confirmed the structural phase transitions for all of them. Cation-dependent magnetic ordering with T_c values up to 92 K and thermal magnetic hysteresis near room temperature (RT) from 264 to 363 K were observed.

Compounds **1**−**4** were synthesized as single crystals from slow evaporation of the mother liquor containing $MnCl_2{\cdot}4H_2O$, NaN_3, and $(CH_3)_nNH_{4-n}Cl$ in the ratio of Mn^{2+}:N_3^-:$(CH_3)_nNH_{4-n}^+$ = 1:5:5 under a nitrogen atmosphere. Compared to the reported preparation of **4**,[16] the present method is much simpler, and the extremely toxic gaseous hydrazoic acid (HN_3) is avoided. According to this general synthetic method, more materials with different amine cations can be synthesized.

Since **1**−**4** undergo a phase transition near RT, as confirmed by thermal analyses and magnetic measurements (vide infra), their crystal structures were measured at different temperatures (173−320 K for **1**, 173 and 323 K for **2**, 173−393 K for **3**, and 173 and 333 K for **4**, respectively, Tables S2 − S4). For **1**, the space groups for both the low-temperature (LT) and high-temperature (HT) phases are $P2_1/c$, but the a and c axes are switched. For **2**, the space groups differ greatly for the two phases, namely orthorhombic $Cmca$ for the HT phase and monoclinic $P2_1$ for the LT phase. Interestingly for **3**, a phase

Received: July 25, 2013
Published: October 16, 2013

dx.doi.org/10.1021/ja407654n | J. Am. Chem. Soc. 2013, 135, 16006−16009

transition occurs at two different temperatures. Upon warming from 173 K, the space group of **3** changes from $P2_1/c$ of the LT phase to $C2/c$ of the IT (intermediate-temperature) phase, and to $R\bar{3}m$ of the HT phase. As for **4**, although the phase transition was reported previously, the HT structure was not determined, and the LT structure was solved in the noncentrosymmetric space group $P2_1$.[16] We solved the HT structure in the space group $Pm\bar{3}m$ and its LT structure in the central space group $P2_1/m$.

As shown in Figures 1 and S1–S2, all compounds exhibit a distorted perovskite-type structure: the Mn^{2+} ions are

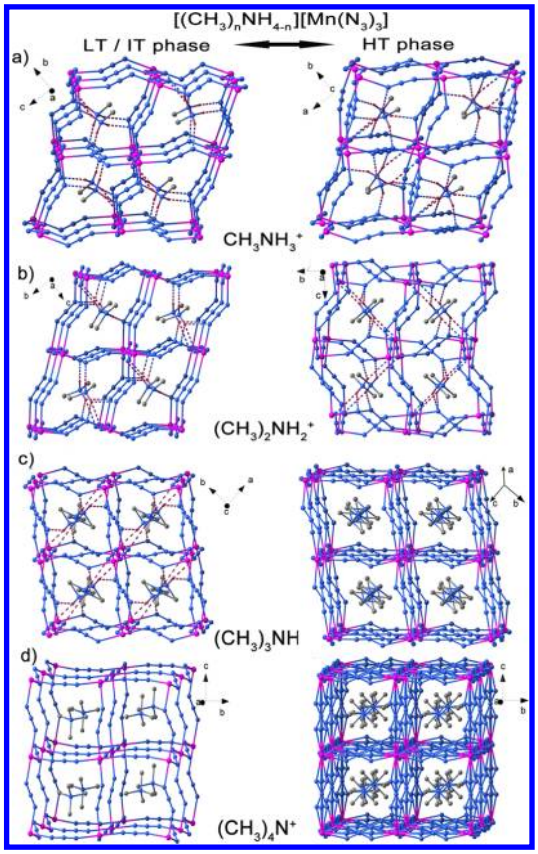

Figure 1. Structures of different phases of **1**–**4**. The LT and HT phases are shown for **1**, **2**, and **4**, and the IT and HT phases are shown for **3**. The dashed lines represent the N–H···N hydrogen bonds between the cations and the azides.

connected by the end-to-end (*EE*) azides to form the 3D architecture with a simple (6,6) topology, while the $(CH_3)_nNH_{4-n}^+$ cations reside in the cavities of the Mn^{2+}-N_3^- network, forming rich N–H···N hydrogen bonds with the terminal N atoms of the azides for **1**–**3** (Table S6). During the phase transition, the differences between the LT and HT structures of **1** and LT and IT structures of **3** are small compared to that of **2** which undergoes a dramatic modification of the structure. Remarkably, as in the formate analogues, disorder was found in the HT structures of **3** and **4**, not only for the cations in the cavity but also for their whole Mn^{2+}-N_3^- lattice, where all azide bridges were disordered in two and four positions for **3** and **4** (Figure 1c,d). The volume of one formula unit $AMn(N_3)_3$ increases monotonously with the size of the cations from **1**–**4**, which correlates with the trend in the critical temperatures of the magnetic ordering of **1**–**4**.

The driving force of the phase transitions for **1**–**4** is not obvious. The N–H···N hydrogen bonds may be responsible as found for the formate analogs.[15] The relatively high symmetry of the $(CH_3)_3NH^+$ and $(CH_3)_4N^+$ cations may also be of relevance as the symmetry of these disordered cations is compatible with the symmetry of the space groups of the HT phases. In fact, the entire frameworks of **1**–**4** are quite flexible, which is very unique among coordination polymers[18] and comparable to the pure inorganic perovskite compounds.[10] Not only does the flexible lattice allow for the incorporation of the cations of different sizes and shapes, it can be adjusted at different temperatures.

To detect the thermally induced phase transitions in **1**–**4**, differential scanning calorimetry (DSC) measurements were performed at different temperature sweep rates (Figures 2 and

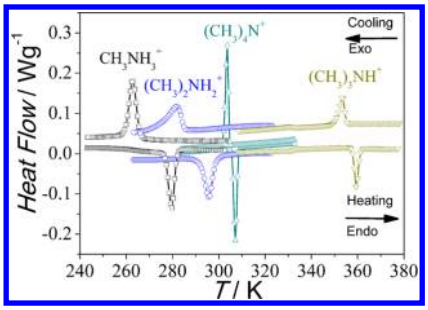

Figure 2. DSC curves of **1**–**4** at 1 K·min^{-1}. Note that the heat flows for **1** and **2** were enlarged by a factor of 5 for clarity.

S3–S6, Table S7). As shown in Figure 2, upon heating/cooling at 1 K·min^{-1}, sharp heat anomalies of endothermic/exothermic peaks were observed at ~280/263, 296/282, 359/354, and 307/304 K for **1**–**4**, respectively. The corresponding ΔH values were estimated to be 1.10/−1.39, 1.21/−1.23, 3.14/−2.86, and 5.71/−5.80 kJ·mol^{-1} for **1**–**4**. The observed thermal hysteresis is nearly sweep rate independent for **1** and **2**, whereas it increases slightly with increasing temperature sweep rates for **3** and **4**. At 1 K·min^{-1}, the width of the hysteresis is 17, 14, 5, and 3 K for **1**–**4**, respectively. The observed sharp peaks and hysteresis indicate the reversible first-order phase transitions for **1**–**4**.[19] For **3**, the hardly noticeable broad peaks were observed at around 331 K (Figure S5). The small thermal effect ($\Delta H \approx$ 0.1 kJ·mol^{-1}) is consistent with the small difference between its LT and IT structures.

The influence of the cations on the magnetic ordering is shown in the field-cooled magnetic susceptibilities of **1**–**4** measured at 10 Oe (Figure 3). Sharp peaks can be observed with the peak temperatures to be around 96, 78, 74, and 66 K for **1**–**4**, respectively. The result for **4** is consistent with the reported 70 K measured at 1 kOe.[16] The critical temperature decreases monotonously with the size of the cations, suggesting the stronger magnetic coupling in a denser structure. To confirm the LT magnetic ordering and the phase transition at around RT, preliminary specific heat capacity (C_p, in heating mode) was measured for **1** on a single crystal from 5 to 300 K (Figure S7). An obvious λ-shaped peak at 92 K and a very sharp peak at 276 K were observed, in good agreement with the above results.

Magnetic measurements were performed for **1**–**4** in the temperature region around the phase transitions with a temperature sweep rate of 1 K·min^{-1} (Figure 4). All the $\chi_M T$ values at the highest temperatures are smaller than the spin-

dx.doi.org/10.1021/ja407654n | J. Am. Chem. Soc. 2013, 135, 16006–16009

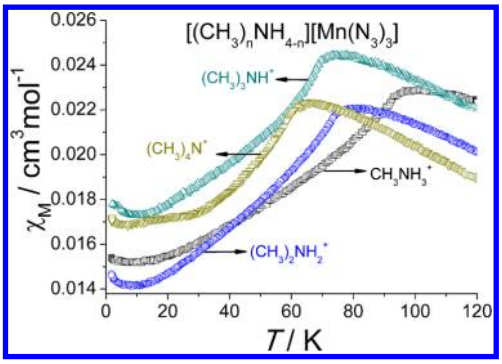

Figure 3. Field-cooled magnetic susceptibilities of **1**−**4** from 2 to 120 K under a dc field of 10 Oe.

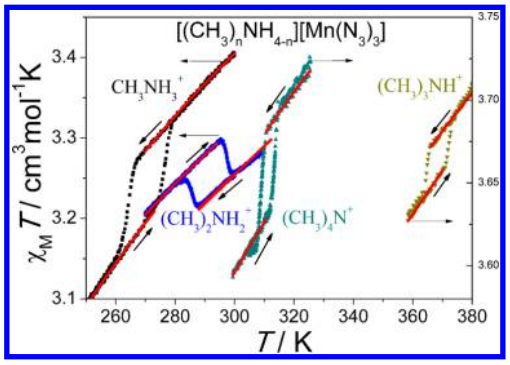

Figure 4. Thermal hysteresis loops of **1**−**4**. The arrows indicate the heating or cooling procedure of the measurements. The red lines are the best-fit with a model for a simple cubic Heisenberg antiferromagnet.

only value (4.375 cm^3 mol^{-1} K) for S = 5/2, confirming the antiferromagnetic coupling transmitted through *EE* azides. Discontinuity and more importantly, thermal hysteresis loops were observed for all compounds with the transition temperatures to be 277/264, 298/286, 363/356, and 309/305 K in the heating/cooling procedure with the hysteresis loop width of 13, 12, 7, and 4 K for **1**−**4**. These results agree well with the DSC measurements. For **1**, **3**, and **4**, the $\chi_M T$ value increases abruptly on changing from the LT (or IT for **3**) to HT phase, which is similar to the normal spin crossover transition.[3] While for **2**, the $\chi_M T$ value decreases on heating during the phase transition and resembles the "reverse spin transition" observed in a cobalt compound.[20] As for **3**, no anomalies were found at the phase transition temperature 331 K (between LT and IT phases) in the $\chi_M T$ curves (Figure S8).

To understand the magnetic behavior of **1**−**4**, magneto-structural relationship is studied. A fitting of the susceptibility data in the region of the hysteresis loops according to a model[21] for a simple cubic Heisenberg antiferromagnet gives the coupling constants J_{LT} and J_{HT} values for the LT and HT phases ($H = -2J\sum_{<i,j>} S_i \cdot S_j$): J_{LT} = −2.42, −2.31, −1.94, and −1.71 K; and J_{HT} = −2.23, −2.45,−1.84 and −1.59 K for **1**−**4**, respectively (g is fixed to 2.02). For **3**, we assume that $J_{LT} = J_{IT}$ since no anomalies were found at the phase transition temperature 331 K. The obtained average magnetic coupling decreases monotonously from **1** to **4**, consistent with the trend of the Néel temperatures. Furthermore, theoretical calculations based on the DFT coupling with the broken-symmetry approach (BS) were carried out for **1**−**4**. The calculations were performed on the model compounds of the dinuclear unit $[Mn_2(N_3)_{10}(\mu\text{-}1,3\text{-}N_3)]^{7-}$ (Figure S9), whose geometrical configurations are based on the actual structures for every unique Mn-N_3^--Mn connections (Supporting Information). The calculated magnetic coupling constants (−2−5 cm^{-1}) are slightly higher than the fitted values. It was found that $|J_{LT}| > |J_{HT}|$ for **1** and **4**, while $|J_{LT}| < |J_{HT}|$ for **2**. This result compares well with the experiment results. As for **3**, the calculation did not give a straightforward conclusion. Also, the $|J|$ values at 173 K for **1** are the largest, consistent with its highest Néel temperature. Due to the very complicated structural alterations during the phase transition, we cannot relate the change of the magnetic coupling to one specific structural parameter, such as the Mn−N−N bond angles and the Mn−NNN−Mn dihedral angles. Such a correlation has been found to be the reason of the thermal hysteresis observed in a dinuclear Ni^{2+}-N_3^- compound.[22]

Because of the noncentrosymmetric space group of the LT phase of **2**, electric ordering might be observed for its LT phase. Since its single crystals crack during the phase transition, powder sample of **2** in the form of disc was used for the preliminary dielectric constant measurement. As can be seen from Figure S10, the signals are quite noisy, and no striking dielectric anomalies were found.

Despite the absence of electric ordering, compounds **1**−**4** are remarkable in several aspects. First, the magnetic bistability originates from modification of the magnetic coupling induced by the phase transition of the flexible framework. This mechanism differs greatly from the existing ones, such as the spin crossover between the high- and low-spin states of a transition-metal center,[3] the metal−metal charge transfer of the cyano-bridged compounds,[4] the monomer−dimer transition of the organic radicals,[5−7] the spin-Peierls-type transition,[8] the modification of the metal's coordination environments of some Ni^{2+} and Cu^{2+} compounds,[9a−d] and the quenching of the orbital angular momentum of a cobalt center.[9e] In the similar $[(CH_3)_2NH_2][M(HCOO)_3]$ compounds, the structural phase transition at around 150−185 K might also modify the magnetic interaction, which is, however, not detectable due to the weak magnetic coupling transmitted through formate. Second, **1**−**4** are actual antiferromagnets with relatively high ordering temperatures for the molecular magnets. This distinctive feature differs from the normal paramagnetic nature of the reported bistable system, where the magnetic coupling is either very weak or restrained in a low-dimensional system. The magnetic ordering might open another physical channel as suggested by the multiferroics in the formate analogs.[15] In this sense, this series of compounds are similar to the cyano-bridged 3D compounds, where photoinduced magnetic ordering can be achieved at low temperature.[23] Finally, both the critical temperatures for the magnetic ordering and hysteretic magnetic bistability of **1**−**4** are cation dependent and increase dramatically compared to that of the formato-bridged analogs. The Néel temperatures increase nearly 10 times, reaching the liquid nitrogen temperature. At the same time, the structural phase transition temperatures are in the vicinity of RT, which increases the possibility for more practical applications of these functional materials.

In summary, we have demonstrated the cation-dependent magnetic ordering and hysteretic magnetic bistability in a series of flexible magnetic MOFs of the perovskite-type structure. Our results suggest an alternative approach for the construction of magnetic bistable materials. As the perovskite structure and its flexibility are retained for different cations, future efforts will be

dx.doi.org/10.1021/ja407654n | J. Am. Chem. Soc. 2013, 135, 16006−16009

aimed at materials with different metal ions and template cations with new physical properties.

■ ASSOCIATED CONTENT

Supporting Information

Experimental details and characterization data. This material is available free of charge via the Internet at http://pubs.acs.org

■ AUTHOR INFORMATION

Corresponding Authors

weihaiyan@njnu.edu.cn
wangxy66@nju.edu.cn

Author Contributions

§These authors contributed equally.

Notes

The authors declare no competing financial interest.

■ ACKNOWLEDGMENTS

We thank the Major State Basic Research Development Program (2013CB922102), NSFC (91022031, 21021062, 21101093) and the NSF of Jiangsu province (BK2011548) for financial assistance.

■ REFERENCES

(1) (a) Kahn, O.; Martinez, C. J. *Science* **1998**, *279*, 44. (b) Kahn, O. *Chem. Br.* **1999**, *35*, 24.

(2) Sato, O.; Tao, J.; Zhang, Y. Z. *Angew. Chem., Int. Ed.* **2007**, *46*, 2152.

(3) (a) Gütlich, P.; Goodwin, H. A. *Top. Curr. Chem.* **2004**, *233*, 1. (b) *Spin-Crossover Materials-Properties and Applications*; Halcrow, M. A., Ed.; John Wiley & Sons: Hoboken, NJ, 2013.

(4) (a) Hendrickson, D. N.; Pierpont, C. G. *Top. Curr. Chem.* **2004**, *234*, 63. (b) Hilfiger, M. G.; Chen, M.; Brinzari, T. V.; Nocera, T. M.; Shatruk, M.; Petasis, D. T.; Musfeldt, J. L.; Achim, C.; Dunbar, K. R. *Angew. Chem., Int. Ed.* **2010**, *49*, 1410. (c) Sessoli, R. *Nat. Chem.* **2010**, *2*, 346. (d) Ohkoshi, S. I.; Tokoro, H. *Acc. Chem. Res.* **2012**, *45*, 1749. (e) Hoshino, N.; Lijima, F.; Newton, G. N.; Yoshida, N.; Shiga, T.; Nojiri, H.; Nakao, A.; Kumai, R.; Murakami, Y.; Oshio, H. *Nat. Chem.* **2012**, *4*, 921.

(5) (a) Fujita, W.; Awaga, K. *Science* **1999**, *286*, 261. (b) Brusso, J. L.; Clements, O. P.; Haddon, R. C.; Itkis, M. E.; Leitch, A. A.; Oakley, R. T.; Reed, R. W.; Richardson, J. F. *J. Am. Chem. Soc.* **2004**, *126*, 8256. (c) Fujita, W.; Awaga, K.; Kondo, R.; Kagoshima, S. *J. Am. Chem. Soc.* **2006**, *128*, 6016. (d) Lekin, K.; Winter, S. M.; Downie, L. E.; Bao, X. Z.; Tse, J. S.; Desgreniers, S.; Secco, R. A.; Dube, P. A.; Oakley, R. T. *J. Am. Chem. Soc.* **2010**, *132*, 16212.

(6) (a) Itkis, M. E.; Chi, X.; Cordes, A. W.; Haddon, R. C. *Science* **2002**, *296*, 1443. (b) Hicks, R. G. *Nat. Chem.* **2011**, *3*, 189. (c) Miller, J. S. *Angew. Chem., Int. Ed.* **2003**, *42*, 27.

(7) (a) Matsumoto, S.; Higashiyama, T.; Akutsu, H.; Nakatsuji, S. *Angew. Chem., Int. Ed.* **2011**, *50*, 10879. (b) Nishimaki, H.; Ishida, T. *J. Am. Chem. Soc.* **2010**, *132*, 9598.

(8) (a) Jeannin, O.; Clérac, R.; Fourmigué, M. *J. Am. Chem. Soc.* **2006**, *128*, 14649. (b) Setifi, F.; Benmansour, S.; Marchivie, M.; Dupouy, G.; Triki, S.; Sala-Pala, J.; Salaün, J. Y.; Gómez-García, C. J.; Pillet, S.; Lecomte, C.; Ruiz, E. *Inorg. Chem.* **2009**, *48*, 1269. (c) Nihei, M.; Tahira, H.; Takahashi, N.; Otake, Y.; Yamamura, Y.; Saito, K.; Oshio, H. *J. Am. Chem. Soc.* **2010**, *132*, 3553. (d) Duan, H. B.; Chen, X. R.; Yang, H.; Ren, X. M.; Xuan, F.; Zhou, S. M. *Inorg. Chem.* **2013**, *52*, 3870.

(9) (a) Panthou, F. L.; Belorizky, E.; Calemczuk, R.; Luneau, D.; Marcenat, C.; Ressouche, E.; Turek, P.; Rey, P. *J. Am. Chem. Soc.* **1995**, *117*, 11247. (b) Venkataramani, S.; Jana, U.; Dommaschk, M.; Sönnichsen, F. D.; Tuczek, F.; Herges, R. *Science* **2011**, *331*, 445. (c) Ma, H.; Petersen, J. L.; Young, V. G.; Yee, G. T.; Jensen, M. P. *J. Am. Chem. Soc.* **2011**, *133*, 5644. (d) Wäckerlin, C.; Tarafder, K.; Girovsky, J.; Nowakowski, J.; Hählen, T.; Shchyrba, A.; Siewert, D.; Kleibert, A.; Nolting, F.; Oppeneer, P. M.; Jung, T. A.; Ballav, N. *Angew. Chem., Int. Ed.* **2013**, *52*, 4568. (e) Juhász, G.; Matsuda, R.; Kanegawa, S.; Inoue, K.; Sato, O.; Yoshizawa. *J. Am. Chem. Soc.* **2009**, *131*, 4560.

(10) Jona, F.; Shirane, G. *Ferroelectric Crystals*; Pergamon: New York, 1962.

(11) Wang, J.; Neaton, J. B.; Zheng, H.; Nagarajan, V.; Ogale, S. B.; Liu, B.; Viehland, D.; Vaithyanathan, V.; Schlom, D. G.; Waghmare, U. V.; Spaldin, N. A.; Rabe, K. M.; Wuttig, M.; Ramesh, R. *Science* **2003**, *299*, 1719.

(12) (a) Jin, S.; Tiefel, T. H.; McCormack, M.; Fastnacht, R. A.; Ramesh, R.; Chen, L. H. *Science* **1994**, *264*, 413. (b) Schiffer, P.; Ramirez, A. P.; Bao, W.; Cheong, S. W. *Phys. Rev. Lett.* **1995**, *75*, 3336.

(13) Zhang, W.; Cai, Y.; Xiong, R. G.; Yoshikawa, H.; Awaga, K. *Angew. Chem., Int. Ed.* **2010**, *49*, 6608.

(14) (a) Wang, X. Y.; Gan, L.; Zhang, S. W.; Gao, S. *Inorg. Chem.* **2004**, *43*, 4615. (b) Wang, Z. M.; Zhang, B.; Otsuka, T.; Inoue, K.; Kobayashi, H.; Kurmoo, M. *Dalton Trans.* **2004**, 2209. (c) Wang, X. Y.; Wang, Z. M.; Gao, S. *Chem. Commun.* **2008**, 281.

(15) (a) Jain, P.; Dalal, N. S.; Toby, B. H.; Kroto, H. W.; Cheetham, A. K. *J. Am. Chem. Soc.* **2008**, *130*, 10450. (b) Jain, P.; Ramachandran, V.; Clark, R. J.; Zhou, H. D.; Toby, B. H.; Dalal, N. S.; Hroto, H. W.; Cheetham, A. K. *J. Am. Chem. Soc.* **2009**, *131*, 13625. (c) Ramesh, R. *Nature* **2009**, *461*, 1218. (d) Besara, T.; Jain, P.; Dalal, N. S.; Kuhns, P. L.; Reyes, A. P.; Kroto, H. W.; Cheetham, A. K. *Proc. Natl. Acad. Sci. U.S.A.* **2011**, *108*, 6828. (e) Fu, D. W.; Zhang, W.; Cai, H. L.; Zhang, Y.; Ge, J. Z.; Xiong, R. G.; Huang, S. D.; Nakamura, T. *Angew. Chem., Int. Ed.* **2011**, *50*, 11947. (f) Thomson, R. I.; Jain, P.; Cheetham, A. K.; Carpenter, M. A. *Phys. Rev. B* **2012**, *86*, 214304.

(16) (a) Mautner, F. A.; Cortés, R.; Lezama, L.; Rojo, T. *Angew. Chem., Int. Ed.* **1996**, *35*, 78. (b) Mautner, F. A.; Hanna, S.; Cortés, R.; Lezama, L.; Barandika, M. G.; Rojo, T. *Inorg. Chem.* **1999**, *38*, 4647.

(17) (a) Bushmarinov, I. S.; Nabiev, O. G.; Kostyanovsky, R. G.; Antipin, M. Y.; Lyssenko, K. A. *CrystEngComm* **2011**, *13*, 2930. (b) Wang, C. F.; Dai, G. L.; Jin, Z. N.; He, Z. C. *Z. Anorg. Allg. Chem.* **2012**, *638*, 1340.

(18) (a) Horike, S.; Shimomura, S.; Kitagawa, S. *Nat. Chem.* **2009**, *1*, 695. (b) Coronado, E.; Espallargas, G. M. *Chem. Soc. Rev.* **2013**, *42*, 1525.

(19) *Liquid Crystals: Experimental Study of Physical Properties and Phase Transitions*; Kumar, S., Ed.; Cambridge University Press: Cambridge, U.K., 2000; pp 246−249.

(20) Hayami, S.; Shigeyoshi, Y.; Akita, M.; Inoue, K.; Kato, K.; Osaka, K.; Takata, M.; Kawajiri, R.; Mitani, T.; Maeda, Y. *Angew. Chem., Int. Ed.* **2005**, *44*, 4899.

(21) Rushbrooke, G. S.; Wood, P. *J. Mol. Phys.* **1958**, *1*, 257.

(22) Leibeling, G.; Demeshko, S.; Dechert, S.; Meyer, F. *Angew. Chem., Int. Ed.* **2005**, *44*, 7111.

(23) (a) Sato, O. *Acc. Chem. Res.* **2003**, *36*, 692. (b) Ohkoshi, S. I.; Tokoro, H. *Acc. Chem. Res.* **2012**, *45*, 1749.